Experimental study of blockage of monochromatic waves by counter currents

by
I. K. Suastika

September 1999

Faculty of Civil Engineering and Geosciences
Delft University of Technology

Table of contents

1. Introduction

Blockage of waves by a current can occur if waves are propagating on a spatially varying opposing current in which the velocity is increasing in the wave propagation direction. The ongoing waves become shorter and steeper while they are propagating against the current. Blocking occurs at the location where the opposing current strength is the same as the effective wave energy transport velocity, the intrinsic wave group velocity. This implies that upstream of this location, the blocking point, there is no propagation of wave energy.

A question that immediately arises is what happens with the ongoing wave energy. The theory suggests that the ongoing waves will break before reaching the blocking point due to steepening of the waves. However, other mechanisms than wave breaking may also play an important role in the wave energy dissipation such as energy dissipations due to wave interactions with the turbulence and due to viscous effects. Another possibility is that the ongoing wave energy may be partially reflected at the blocking point. Some earlier studies (e.g. Long et al [1993]) have reported some evidence of wave reflection in blocking situations.

The present study aims to investigate experimentally the phenomena of wave breaking and/or wave reflection in blocking situations. For this purpose a novel experimental arrangement has been designed and implemented in a laboratory flume. Previous laboratory studies utilized a constant discharge (Q) and a varying cross section (A) to obtain a longitudinal velocity gradient. This has the disadvantage that the effects of nonuniform cross-section and non-uniform velocity are mixed. In the present study, it was decided to use a constant cross-section and a non-uniform discharge, to be obtained by withdrawal of water through a perforated false bottom.

1.1. Earlier studies

Some earlier studies on wave-current interactions have reported the existence of the blocking phenomenon. Lai et al. [1989] investigated in their laboratory study the kinematics of the 'strong' wave-current interaction, referring the strong interactions as the changes of the waves by the currents detectable within a few wavelengths. Their spatially varying currents were achieved by using an impermeable false sloping bottom with a minimum water depth of 45.0 cm over the top of the false bottom and an operating water depth of 75.0 cm outside the false bottom. In this series of experiments, the maximum opposing current velocity over the top of the false bottom was about 13.0 cm/s for the gentle breaking, and about 23.0 cm/s for the more violent one. For the case of non-breaking waves in the steady state condition, the experimental data confirm the kinematic conservation of the waves. Further, the measured wave number and the inferred intrinsic frequency follow the linear dispersion relationship very well, and the variations of the wave number along the tank seem to follow the theoretical curve well. For the case of breaking waves, the theoretical blockage limit of $U/C_0 = 1/4$ is confirmed, where U is the opposing current velocity and C_0 is the deep water wave speed in the absence of a current.

In contrast to the theory that the waves will break before reaching the blocking location, the reflection theory suggests that, instead of breaking, the waves are reflected at this location. This theory offers the possibility of the occurrence of double reflection and 'trapping' of the waves in the area of strong current gradients. The laboratory study of Long et al. [1993] was aimed at investigating these phenomena. Their experiments were conducted in the same tank as used by Lai et al. [1989]. Since the continuous wave experiment failed in detecting the waves to be reflected, envelope soliton waves were used, which can maintain their integrity over a relatively long period. Since solitons are transient waves, Fourier transforms are not appropriate for the analysis. Instead of these, wavelet analysis was used.

As a reference, the propagation of soliton in still water was considered. In this case, as nothing extraordinary occurred, the soliton passed through each station uneventfully. The propagation speed derived from the arrival time vs. distance curves follow the linear dispersion relationship well.

The second case was a partial blocking in which the maximum opposing current velocity over the top of the false bottom was 23.0 cm/s, and the third a total blocking in which the maximum opposing current velocity over the top of the false bottom was 35.0 cm/s. In the second case, only the forerunner of the soliton could pass through the maximum opposing current as it is of lower frequency. In the third case, there was a local high energy density level observed in the zone of strong velocity gradient, which was of relatively long period, indicating the existence of trapping as dictated by the theory.

Sakai et al. [1986] studied experimentally the transformation of irregular waves by opposing currents. They derived a formulation for the wave decay in which the energy flux was calculated by the linear long wave theory and the dissipation of breaking was approximated by the dissipation of a propagating bore. This formulation was applied to each component of the irregular waves resulting in wave height distribution as function of water depth. They found that the transformation of irregular waves by currents is characterized by the dimensionless discharge per unit width and the deep water wave steepness. This is qualitatively the same as that for regular waves. Further, they found that, due to the presence of opposing currents, the surf zone is moved offshore and the wave decay occurred more promptly after breaking.

The experimental study of Chawla and Kirby [1998] was aimed to investigate wave blocking by currents and to verify whether a bore dissipation model can be used to simulate current limited wave breaking. Their longitudinal current gradient was achieved by varying the cross sectional area of the flume which was established by using a false wall. They found that the predictions of energy decay from the bore model are reasonably accurate, and that amplitude dispersion plays an important role in wave blocking. For relatively large amplitude waves, they also found that wave energy shifts to lower frequency due to side band instabilities, and the waves were not blocked in this case as predicted by the model.

1.2. Note on waves being reflected at the blocking point

Previous studies (e.g. Long et al. [1993]) have mentioned wave reflection in situations of wave blocking. If there is wave energy being reflected at the blocking point, we may wonder what kind of waves will be generated at the blocking point. An investigation of the dispersion relation (see Figure 2) reveals that we may identify two kinds of reflected waves. First, reflected waves given by solution r_1 of the dispersion relation, and second those given by solution r_2. Solution r_1 represents waves with forms and effective energy transport in the downstream direction ($c+U<0$, $cg + U <0$), and solution r_2 represents those with forms propagating upstream but effective energy transport in the downstream direction ($c+U>0$, $cg + U <0$).

First, consider the situation where the wave train is approaching the blocking point and the steady state condition has not been achieved. Due to interactions with the current, the wave length becomes shorter, and at the blocking point it reaches its minimum value. If there are waves being reflected at the blocking point, it is most likely that only waves r_2 will be generated. An argument is that while waves are reflected at the blocking point there exists only a single solution (k, σ) at the blocking point. This will be fulfilled if only waves r_2 are being reflected at the blocking point. Waves r_1 is unlikely to be generated since this implies discontinuity in the wave number.

Second, in the steady state condition there applies for the total wave field that $c_g + U$ is zero at the blocking point. This condition will be fulfilled if the wave field only consists of the incoming waves and waves r_2. If waves r1 were present, $c_g + U$ of the total wave field at the blocking point is negative. This implies that the blocking point must propagate downstream, which is not the case.

The arguments above exclude the generation of waves r_1 in blocking situations, and if there are waves being reflected at the blocking point then only waves r_2 will be generated.

2. Experimental arrangement

In order to make further studies of wave blocking, the occurrence of breaking and/or reflection, and the damping of the ongoing waves, experiments have been conducted at the Laboratory of Fluid Mechanics of the Faculty of Civil Engineering and Geosciences, Delft University of Technology, The Netherlands. Therefore, a novel experimental arrangement has been designed and implemented.

The key to the design is a 12 m long measurement section in the central portion of a 40 m long flume in which discharge entering at one end is gradually withdrawn through the bottom and brought to zero at the other end. The final lay-out is shown in Figure 1 with side view, plan view and cross-section of the flume with installations.

The flume is equipped with a wave generator at one end (to the right in the longitudinal view and plan view), with permeable wave damping material at the opposite end where also a flow of water could be let into the flume with controlled discharge. Large-scale turbulence and swirling motions in the inflowing current were dampened by a honeycomb. At both ends the full flume width (0.8

m) and height (1.0 m) were available to the waves and the current, respectively, but with the aid of a vertical false wall and a false bottom the available width and height were reduced to 0.4 m and 0.7 m in the measurement section in the middle part of the flume.

In order to obtain a smooth inflow, both the false bottom and the false wall at the upstream end of the flume were streamlined, forming a gradual decrease of the available cross-section in the flow direction. At the upwave end of the flume, a concreted sloping bottom formed a gradual transition between the original flume bottom and the false bottom in the measurement section. The false wall at that end was not streamlined but instead acted as a splitter wall, so as to allow undisturbed wave propagation into the measurement section. The waves propagating into the dummy half of the flume were dissipated there on a 1:10 gravel spending beach.

The 12 m long measurement section was divided into six compartments of 2 m length each, with a false perforated bottom allowing withdrawal of discharge through this bottom into the adjacent dummy half of the flume, which in turn acted as a sump for six 10.0 cm inner diameter suction pipes, one for each compartment. (Along the entire 12 m long measurement section, the vertical false wall reached only to the false bottom, allowing lateral flow of water from underneath the false bottom into the adjacent dummy half of the flume; see cross-section A - A'.) Each suction pipe was mounted vertically in the dummy half of the flume and connected to a horizontal conduit provided with a control valve and discharge meter. These six conduits in turn led via two manifolds to two pumps from which the water was returned through two pressure pipes and delivered to the upstream end of the flume.

In order to better control the longitudinal discharge variations (i.e., to prevent longitudinal short-circuiting), the six 2 m long compartments were separated by vertical plywood plates normal to the flume length axis, occupying the entire flume cross-section except the reduced area available for the current and the waves. In this manner it was guaranteed that each of the six suction pipes would withdraw water from only the 2 m long compartment adjacent to it.

Downstream of the measurement section with variable discharge a region exists where the discharge and therefore the cross-sectionally averaged current velocity is zero. In this stagnant region, waves are generated by a wave generator, through horizontal translation of a vertical wave paddle. The motion of the paddle is controlled with electronic signals generated by Auke-stir2C, a wave generation package developed within WL|Delft Hydraulics. This package is capable of generating regular waves of different periods and heights, and irregular waves with different target energy spectra, with second - order control to prevent spurious harmonics. It also has an automatic reflection absorption capability.

Capacitance gauges were used to measure the water surface elevation, and Laser Doppler (LDA) and Electromagnetic (EMS) velocity meters for the water particle velocity. In addition, video recordings have been made to show the experimental set - up, to visualise some physical processes occurring in the flume, and to allow quantitative analysis of some visually observable phenomena.

3. Model for blockage of monochromatic waves

The existence of the reflected waves, which have the intriguing properties that their forms are propagating upstream but their energy is being swept downstream by the current, has been observed during our experiments. They have been recorded on video tape. In this paragraph we present a model allowing us to discriminate these reflected waves from the incoming waves.

The model incorporates two basic elements. The first models the amplitude evolution and the second the phase variation for both the incoming and the reflected waves. The calculation of the amplitude evolution is based on the wave action balance in which three kinds of energy dissipation are involved. These are dissipations due to viscous effects, wave breaking and wave - turbulence interactions. The phase variation of the incoming waves is calculated as a phase shift from the reference probe and that for the reflected waves as a phase shift from the blocking point. A description of the amplitude evolution and the phase variation is presented in section 3.1 and 3.2, respectively.

The essence of the model is as follows. The incoming wave train is assumed to evolve according to the wave action balance, dissipating a part of its energy on the way to the blocking point, and once it reaches the blocking point, a part of its energy is reflected at this point. The reflected wave train having been generated at the blocking point is also assumed to evolve according to the wave action balance and to dissipate energy while it is being swept downstream by the current.

The model is a linear one, in the sense that the calculation is performed only on the fundamental wave components. Higher harmonic components are not included. Moreover, wave kinematics are calculated by using the linear theory and data fitting is done on the data obtained from the stagnant region until the location of the blocking point which is also predicted by the linear theory.

3.1 Amplitude evolution of the incoming and reflected waves

The amplitude evolution of both the incoming and reflected waves is described by the wave action balance as

$$\frac{d}{dx}\left[\left(c_g + U\right)\frac{E}{\sigma}\right] + \frac{D}{\sigma} = 0 \tag{1}$$

where U : mean current velocity

E : wave energy density

D : dissipation per unit area wave field

σ : intrinsic wave frequency

c_g : intrinsic wave group velocity

Three mechanisms of wave energy dissipation are incorporated: viscous effects, wave breaking and wave - turbulence interactions. The dissipation due to viscous effects is estimated using Hunt's formulation [1952] which can be expressed as

$$D_H = 2K\left(c_g + U\right)E \tag{2}$$

The term K in eq. (2) represents a damping modulus equal to

$$K = \left(\frac{2k}{h}\right)\left(\frac{\upsilon}{2\sigma}\right)\left(\frac{kb + \sinh 2kh}{2kh + \sinh 2kh}\right) \tag{3}$$

where b : the channel width

h : water depth

k : wave number

ν : kinematic viscosity of water

The dissipation due to wave breaking is calculated according to the formulation of Battjes- Janssen bore dissipation model [Battjes and Janssen, 1978] as

$$D_{BJ} = C_B \frac{1}{\pi}\left(\frac{8}{\rho h}\right)^{\frac{1}{2}} kE^{\frac{3}{2}} \tag{4}$$

where C_B is a non-dimensional parameter associated with dissipation due to wave breaking.

The wave energy dissipation due to wave - turbulence interactions is one of those processes that is not easy to model since this requires a proper technique to separate the fluctuating field into wave - induced and turbulent parts. However, Rosenthal [1989] has proposed an expression for the wave energy dissipation due to wave - turbulence interactions without making this separation. He considered progressive waves in still water, and derived a dissipation formulation by including the Stokes drift in the expression for the turbulent diffusion. Schneggenburger [1998] has used his formulation in the spectral wave modeling of wind waves and found a good agreement with some observations.

In the present study we use the formulation of Rosenthal to model the wave energy dissipation due to wave - turbulence interactions. For deep water cases, this is represented as

$$D_R = \rho \frac{S}{4} g k^4 a^4 \tag{5}$$

where S is turbulent eddy viscosity. The order of magnitude of the eddy viscosity S is estimated as

$$S \approx u_* h \tag{6}$$

where

u_*: friction velocity

h: water depth

Eq. (6) can be rewritten as

$$S(x) = C_T U(x) h = C_T q(x) \tag{7}$$

where

U: mean velocity

q: discharge per unit width

C_T: non-dimensional parameter associated with energy dissipation due to wave - turbulence interaction

By using the deep water dispersion relation, and, to first order, E is proportional with a^2, eq. (5) can be represented as

$$D_R = C_T \frac{qk^4 E^2}{\rho g} \tag{8}$$

The wave action balance, eq (1) and the energy dissipation formulations, eqs. (2), (4) and (8) are applied for both the incoming and the reflected waves.

3.2. Phase variation of the incoming and reflected waves

In addition to the amplitude evolution, the phase variation of both the incoming and reflected waves has to be modeled properly. The phase of the incoming waves at a given position along the flume is calculated as a phase shift from the reference probe. This is represented as

$$\psi_i(x) = \int_{x_0}^{x} k_i dx \tag{9}$$

where ψ : phase shift

k : wave number

x : position along the flume

x_0 : reference position

subscript i refers to incoming wave component

The local wave number k is calculated from

$$\omega = \left(gk \tanh kh\right)^{\frac{1}{2}} + kU \tag{10}$$

using the given (constant) value of ω and the local values of h and U.

The phase variation of the reflected waves can not be referred to the reference probe, since this is located in the stagnant region where these waves theoretically do not exist. Instead of this, their phase variation is calculated as a phase shift from the blocking point. This is represented as

$$\psi_r(x) = -\int_x^{x_B} k_r dx \tag{11}$$

where x_B is the location of the blocking point and subscript r refers to reflected wave component.

3.3. Wave field as a superposition of incoming and reflected waves

Having modeled the amplitude evolution and the phase variation of both the incoming and reflected waves, we assume now the total wave field as a superposition of incoming and reflected waves as

$$\phi = \phi_i + \phi_r \tag{12}$$

where

$$\phi_i = a_i(x)\exp\left(-i\psi_i(x)\right)$$

$$\phi_r = a_r(x)\exp\left(-i\psi_r(x)\right)$$

where

ϕ : wave field

a : wave amplitude

The surface elevation of the total field η is represented as

$$\eta = \mathrm{Re}\left(\phi\right) \tag{13}$$

Those of the incoming and the reflected component are represented, respectively, as

$$\eta_i = \mathrm{Re}(\phi_i) \tag{14}$$

$$\eta_r = \mathrm{Re}(\phi_r) \tag{15}$$

where Re represents real part of.

4. Least square error data fitting

Having developed a model for the wave field, we utilize a least square error method to be fitted to the experimental data. In the data fitting a number of physical parameters are estimated, which are associated with energy dissipations due to wave breaking C_B and wave - turbulence interactions C_T. (Since the formulation of Hunt for the energy dissipation due to viscous effects has been found to be adequate, see report "Viscous dissipation of monochromatic waves in still water of finite constant depth in a channel of finite width", distributed previously, we do not estimate the parameter C_V, but instead assume this to be equal to one.)

Data fitting is done on the data obtained from the stagnant region up to the blocking point which is predicted by the linear theory. Since the blocking point observed experimentally lies further upstream than that predicted by the linear theory, a part of the ongoing wave energy can pass through the theoretical blocking point. This is incorporated in the model by assuming that only a part of the ongoing wave energy is reflected at the (theoretical) blocking point. This fraction of wave energy being reflected at the (theoretical) blocking point, denoted as F_R, has to be estimated from the data fitting.

First Fourier analysis is performed to the surface elevation data recorded at each station. This results in Fourier components of surface elevation at each station, from which only the fundamental wave component is fitted. We denote the fundamental wave component determined from the experimental data by η_m.

The surface elevation calculated from the model will be denoted by η_s.

We optimize our estimate by minimizing the squared difference between the surface elevation determined from the experimental data and that calculated from the model:

$$s = \sum_j \left(\eta\_m_j - \eta\_s_j\right)^2 \tag{16}$$

where j refers to measurement stations from the stagnant region to the blocking point.

5. Results

We present here the results of the analysis of three tests with monochromatic waves. The absolute wave period in all the three cases is 1.10 s. However their initial wave heights are not the same. These are 0.02, 0.05 and 0.07 m, respectively. For shortness, we shall refer to the case of 1.10 s period and 0.02 m initial height as r1102, and similarly for the others. The opposing current velocity is increasing about linearly, with a cross sectional average velocity (Q/A) of zero at x = 11.0 m to a maximum of 0.55 m/s at x = 23.0 m.

Figure 3a shows the observed and modeled amplitude evolutions of the total wave field for the r1102 test. The observed and modeled phase variations of the total field for this test are shown in Figure 3b while the modeled amplitude evolutions of the incoming and reflected waves are shown in Figure 3c.

Figures 4 and 5 present the same kind of results for tests r1105 and r1107.

Table 1 presents the physical parameters having been estimated from the three tests

	C_B	C_T	F_R [%]
r1102	0.200	0.510	0.98
r1105	0.102	0.197	0.96
r1107	0.109	0.114	1.01

Table 1. Physical parameters C_B and C_T having been estimated from the test r1102, r1105 and r1107.

6. Discussions

The results presented here have shown that the fitted model is capable to reproduce the experimental data fairly well. Both the amplitude evolution and the phase variation of the total field were modeled adequately. Based on the model, we are able to discriminate the reflected waves and the incoming ones. The amplitude evolution of both the incoming and the reflected waves predicted by the model looks sensible. In general, the reflection is very weak; the reflected wave amplitude at the blocking point is about ten percent of that of the incoming one, and it decreases very rapidly in the downstream direction. The physical parameters C_B and C_T were found not constant for waves of different initial steepness. This suggests that the wave steepness influence is overestimated in Rosenthal's model.

7. Conclusions

The fitted model has shown to be capable to reproduce the wave field of monochromatic waves being blocked by a counter current reasonably well, allowing us to discriminate the reflected waves and the incoming waves. However, the model in its present form contains unknown calibration coefficients whose variation requires further study and most likely a reformulation of the dissipation model.

8. Acknowledgment

This study is supported by A L W.

References

Battjes J. A. and Janssen, J. P. F. M., 1978. Energy loss and set - up due to breaking of random waves. Coastal Eng.: 569-587.

Chawla, A. and Kirby, T., 1998. Experimental study of wave breaking and blocking on opposing current. Private communications.

Lai, R. J., Long, S. R., Huang, N. E., 1989. Laboratory studies of wave-current interaction: kinematics of the strong interaction. J. Geophys. Res., 94:16201-16214.

Long, S. R., Lai, R. J., Huang, N. E., Spedding, G. R., 1993. Blocking and trapping of waves in an inhomogeneous flow. Dynamics of atmospheres and oceans, 20: 79-106.

Rosenthal, W., 1989. Derivation of Phillips α - parameter from turbulent diffusion as damping mechanism. In: Radar Scattering from Modulated Wind Waves, G. J. Komen and W. A. Oost, eds., Kluwer Academic Publisher, p. 81 - 88.

Sakai, S., Hiyamizu, K., Saeki, H., 1986. Irregular wave transformation affected by opposing currents. Proc. 20th Coastal Eng. Conf., Taipei, Taiwan, ASCE New York: 1132-1148.

Schneggenburger, C., 1998. Spectral wave modeling with nonlinear dissipation. Ph. D. - thesis, Hamburg University, Germany.

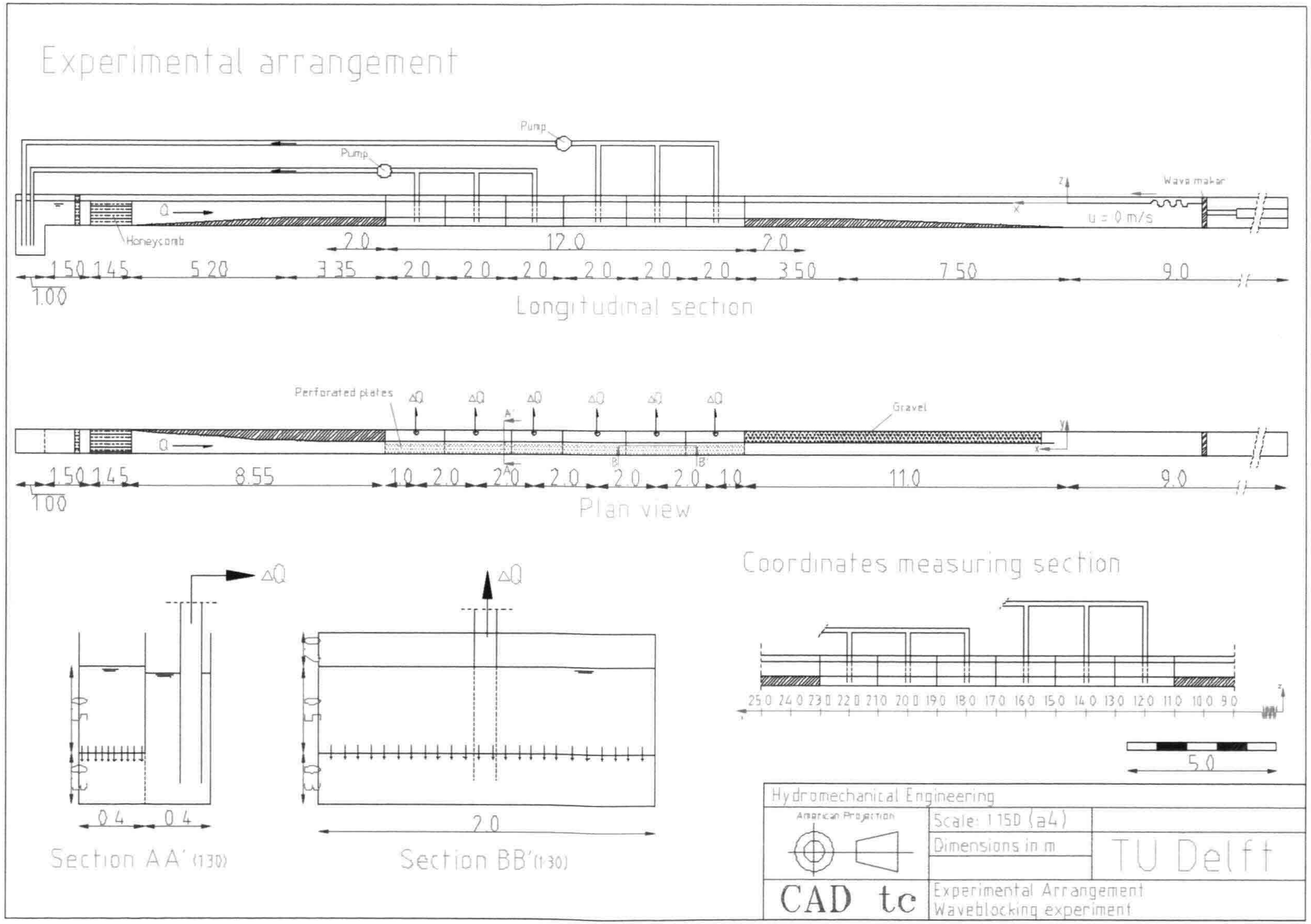

Figure 1. Lay out of the experimental arrangement with side view, plan view and cross-section of the flume with installations.

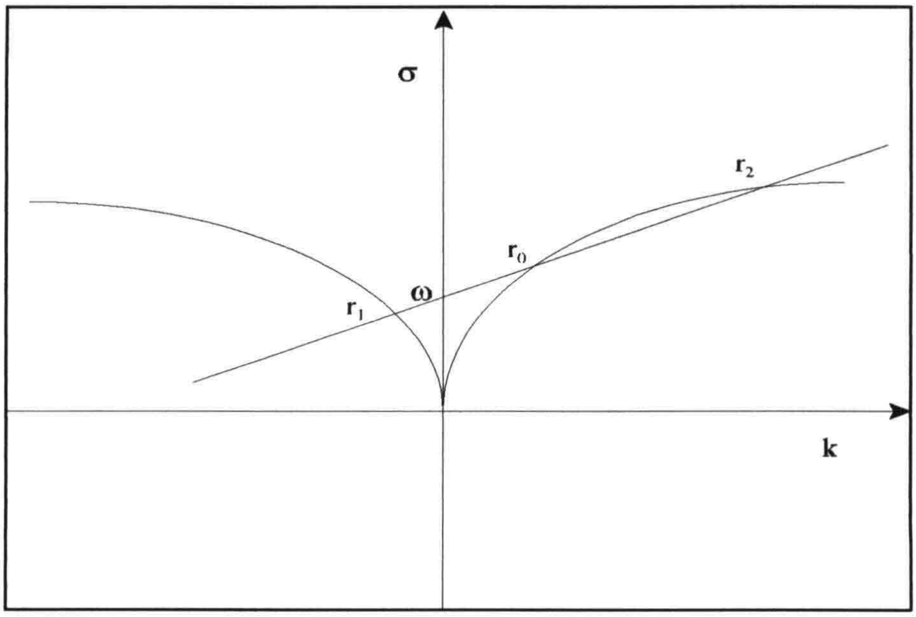

Figure 2. Schematic representation showing three roots of the dispersion relation: r_0 represents the ongoing waves, r_1 waves with phase velocity and effective energy transport in the downstream direction, and r_2 waves with phase velocity in the upstream direction but with effective wave energy transport in the downstream direction.